

# Study on Power Factor of Wireless Power Transfer Systems with Resonance Frequency Mismatch

Helanka WEERASEKARA<sup>†</sup>, Katsuhiko HATA<sup>†</sup>, Takehiro IMURA<sup>†</sup>, and Yoichi HORI<sup>†</sup>

<sup>†</sup> Graduate school of Engineering, The University of Tokyo  
5-1-5, Kashiwanoha, Kashiwa, Chiba, 277-8561, Japan  
E-mail: †weerasekara.helanka18@ae.k.u-tokyo.ac.jp

**Abstract** Wireless Power Transfer (WPT) for Electric Vehicles (EV) is one of an admirable solution to some obstacles of charging EVs. The operation frequency, secondary resonance frequency and primary resonance frequency are assumed to be equal in the previous WPT studies. However, in real WPT system, resonance frequency mismatch occurs, when primary and secondary sides have different resonance frequencies due to inductance and capacitance change. This paper is investigated on the power factor for the wireless power transfer systems with resonance frequency mismatch. The effectiveness of the theoretical analysis has been verified under resonance frequency mismatch condition by experimentally.

**Key words** Wireless power transfer, resonance frequency mismatch, power factor

## 1. Introduction

In recent years, electric vehicle (EV) is considered to be the aspiration for zero emissions while driving. Therefore, the EV appears to be one of the best options for public transportation and has raised the propagation of EV in the market [1], [2]. However, as EV and plug-in hybrid vehicles (PHEV) can perform only short-distance cruising with one charge and has some problems of long charging time [3] [4]. As a method to solve these problems, wireless power transfer (WPT) attracts attention [5]. Currently, in order to improve safety and reliability, the application of WPT technology is researched actively on the survey of automobile manufacturers in charge of road traffic planning [6]. In WPT system, Previous studies have been conducted assuming that the primary side resonance frequency, the secondary side resonance frequency, and the operation frequency is same with each other.

However, in practice, resonance frequency mismatch occurs and the above-mentioned condition can not be applied. Next, the constant variations of actual coils and capacitors are explained. The resonance frequency varies depending on the variation of the elements of the coil and the capacitor. In manufacturing process, errors appear in coil and the capacitors, and the resonance frequency changes. In the environmental change, errors occur in coil and the capacitors due to problems such as temperature, and the coil expands and contracts at high temperature and low temperature repetition. For above matters, using high quality materials and

exclude large errors are some methods to reduce the constant change in the coil and capacitor.

On the other hand, these solutions have some problems too such as high cost, sorting man-hours and also some principle matters. Therefore, it is necessary to analyze the WPT circuit with constant variations in the coil and the capacitor. Furthermore, Transmission efficiency and transmission power characteristics are unique and easy to understand. However, power factor is difficult to understand the characteristics and analyzing of power factor characteristics is necessary for equipment capacity reduction problem too. In this paper, first study about the effectiveness of primary and secondary resonance frequency to power factor by theoretically. Next, analyzed the power factor for WPT systems with resonance frequency mismatch using simulation. Finally, did the measurements on power factor for resonance frequency mismatch for different frequencies.

## 2. WPT circuit analysis on power factor

Wireless power supply is coupled by a magnetic field in the resonance state of the coil and the capacitor, and power transmission is performed. In WPT system, the power is transferred from the transmitting coil to the receiving coil by inducing the voltage in receiving coil from magnetic field generation in transmitting coil as shown in Fig. 1. Many studies have suggested that the resonance frequency of primary side capacitance  $C_1$  and Inductance  $L_1$  should be equal to the secondary resonance frequency as follows [7], [8]:

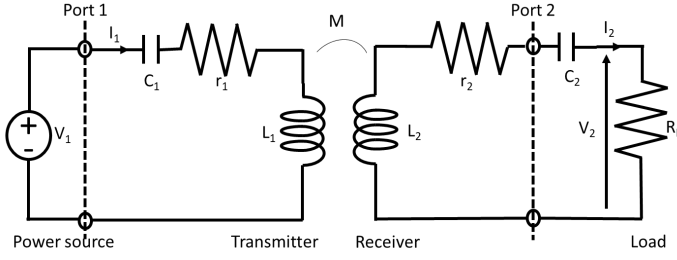


Fig. 1 Circuit diagram of SS type WPT circuit.

$$f_0 = \frac{1}{2\pi\sqrt{L_1 C_1}} = \frac{1}{2\pi\sqrt{L_2 C_2}}. \quad (1)$$

$f_0$ ,  $C_1$ ,  $L_1$  represents the operating source frequency, secondary side capacitance and the inductance respectively. In Fig. 1, output voltage  $V_2$ , input current  $I_1$ , output current  $I_2$  are calculated as shown in (2), (3) and (4) respectively, where  $V_1$ ,  $R_1$ ,  $R_2$ ,  $R_L$ ,  $\omega_0$ ,  $\omega_1$ ,  $\omega_2$ ,  $M$  are input voltage, transmitter coil resistance, receiver coil resistance, load resistance, operating angular frequency, primary resonance angular frequency, secondary resonance angular frequency and mutual inductance of the primary and secondary coil, respectively. Then, input power factor  $\cos \theta_1$  is calculated by (6), expressed as (7).

$$V_2 = R_L I_2. \quad (2)$$

$$I_1 = \frac{\left( R_2 + R_L + j\omega_2 L_2 \left( \frac{\omega_0}{\omega_2} - \frac{\omega_2}{\omega_0} \right) \right) V_1}{\left\{ R_1 + j\omega_1 L_1 \left( \frac{\omega_0}{\omega_1} - \frac{\omega_1}{\omega_0} \right) \right\} \left\{ R_2 + R_L + j\omega_2 L_2 \left( \frac{\omega_0}{\omega_2} - \frac{\omega_2}{\omega_0} \right) \right\} + \omega_0^2 M^2} \quad (3)$$

$$I_2 = \frac{j\omega_0 M V_1}{\left\{ R_1 + j\omega_1 L_1 \left( \frac{\omega_0}{\omega_1} - \frac{\omega_1}{\omega_0} \right) \right\} \left\{ R_2 + R_L + j\omega_2 L_2 \left( \frac{\omega_0}{\omega_2} - \frac{\omega_2}{\omega_0} \right) \right\} + \omega_0^2 M^2}. \quad (4)$$

Primary side active power  $P_{e1}$  and apparent power  $P_{a1}$  are defined as follows:

$$P_{e1} = \text{Re}(V_1 \bar{I}_1), \quad P_{a1} = \sqrt{\left\{ \text{Re}(V_1 \bar{I}_1) \right\}^2 + \left\{ \text{Im}(V_1 \bar{I}_1) \right\}^2} \quad (5)$$

$$\cos \theta_1 = \frac{P_{e1}}{P_{a1}} \quad (6)$$

$\cos \theta_1 =$

$$\left\{ r_1 (r_2 + R_L)^2 + r_1 \omega_2^2 L_2^2 \left( \frac{\omega_0}{\omega_2} - \frac{\omega_2}{\omega_0} \right)^2 + \omega_0^2 M^2 (r_2 + R_L) \right\}$$

$$\sqrt{\left\{ r_1 (r_2 + R_L)^2 + r_1 \omega_2^2 L_2^2 \left( \frac{\omega_0}{\omega_2} - \frac{\omega_2}{\omega_0} \right)^2 + \omega_0^2 M^2 (r_2 + R_L) \right\}^2 + \left\{ -\omega_1 \omega_2^2 L_1 L_2^2 \left( \frac{\omega_0}{\omega_1} - \frac{\omega_1}{\omega_0} \right) \left( \frac{\omega_0}{\omega_2} - \frac{\omega_2}{\omega_0} \right)^2 - (r_2 + R_L) \omega_2 L_2 \left( \frac{\omega_0}{\omega_2} - \frac{\omega_2}{\omega_0} \right) + (r_2 + R_L)^2 \omega_1 L_1 \left( \frac{\omega_0}{\omega_1} - \frac{\omega_1}{\omega_0} \right) \right\}^2} \quad (7)$$

Input power factor is influenced by both primary and secondary side resonance frequency by equation(7). On the

Tab. 1 Parameters of transmitting and receiving coil

Parameter	Transmitter	Receiver
Resistance $R_1, R_2$	1.00 $\Omega$	1.05 $\Omega$
Inductance $L_1, L_2$	617 $\mu\text{H}$	617 $\mu\text{H}$
Coupling coefficient $k$	0.1	
Transmitting gap	300 mm	
Outer diameter	440 mm	
Number of turns	50 turns	

other hand output power factor becomes 1, according to the same calculations as above. Therefore, the simulation and measurements are done for only the input power factor.

### 3. Verification

#### 3.1 Simulation Verification

In order to analyze the relationship of power factor and resonance frequency of the wireless power transfer systems with resonance frequency mismatch, a SS-type WPT circuit calculations are used and the parameters are shown in Tab. 1. Numerical analysis are performed using the transmission efficiency equation obtained in section 2.

Theoretical calculations are done at 5 different values of operating source frequency to obtain, the influence of resonance frequency mismatch to the power factor and shown in Fig. 2. As can be seen from (7), Input power factor is influenced by both primary and secondary side resonance frequency. In Fig. 2 Input power factor is presented using parula color map in which the color yellow represents the larger values. It can be clearly seen from Fig. 2, the yellow color converge towards a point where the primary and secondary side resonance frequency are equal to the operating source frequency.

#### 3.2 Measurement verification

This time the measurement conditions are different from the typical measurements of WPT system because of the resonance frequency mismatch. So, we did the measurements for various resonance frequency mismatch by changing the primary and secondary side capacitance shown in Tab. 2. The coils used for the measurements are shown in Fig. 3 and the parameters of the coils are listed in Tab. 1. In the measurement, the Vector Network Analyzer (VNA, E5061B ENA Series Keysight) was connected to port 1 and port 2 shown in Fig.1, and the primary power factor was measured.

First, the resonance frequency range is selected from 81 kHz to 89 kHz(81 kHz, 83 kHz, 85 kHz, 87 kHz, 89 kHz)that

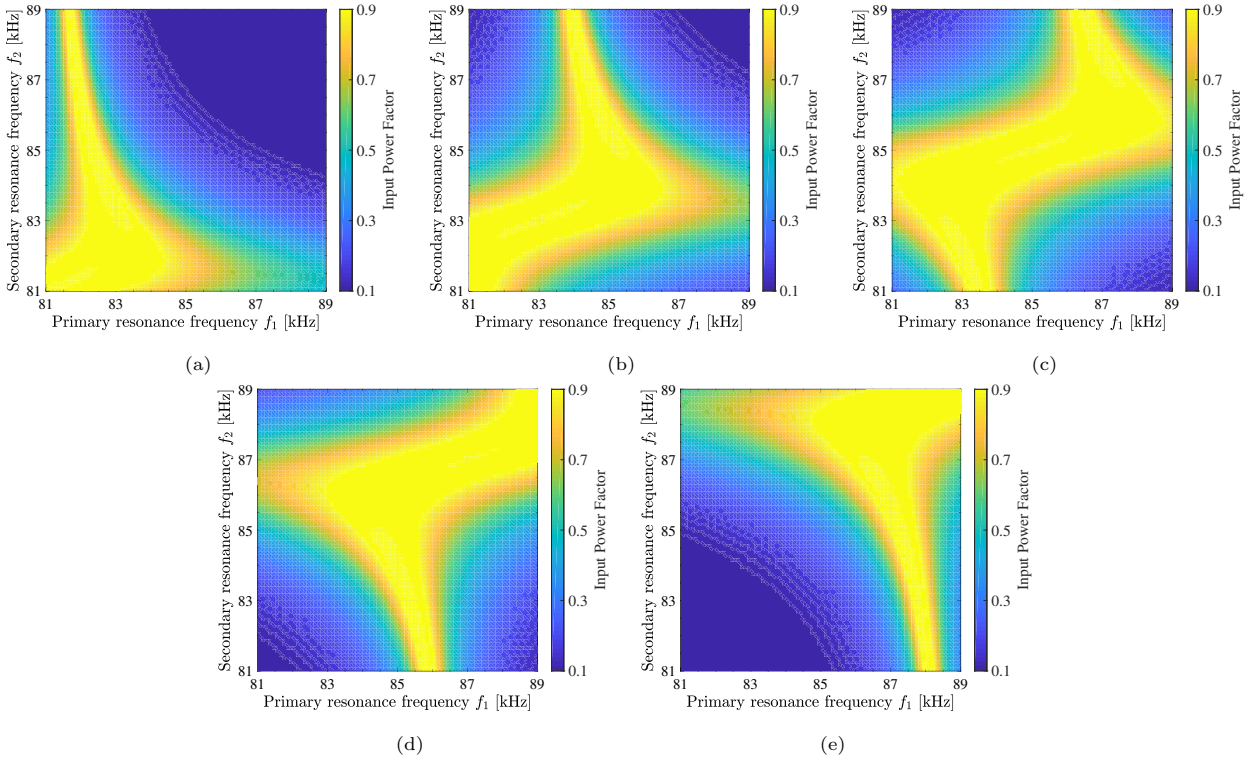


Fig. 2 Theoretical results of transmission efficiency on resonance frequency mismatch.

Tab. 2 Measurement Conditions

$f_1, f_2$ [kHz]	$C_1, C_2$ [nF]
80.9	6.26
82.6	6.02
84.9	5.69
86.5	5.49
89.0	5.18

can be used to verify the Theoretical Calculations. Then, from (8) and (9), the primary and the secondary side capacitance are calculated that corresponds to the above resonance frequency range.  $f_1$  and  $f_2$  are the primary and the secondary resonance frequency in (8) and (9).

$$f_1 = \frac{1}{2\pi\sqrt{L_1 C_1}} \quad (8)$$

$$f_2 = \frac{1}{2\pi\sqrt{L_2 C_2}} \quad (9)$$

The Transmitting and receiving coil is used for verification according to Fig. 3 with the parameters shown in Tab. 1. Fig. 4 shows the circuit measurement result of Transmission efficiency at 81 kHz, 83 kHz, 85 kHz, 87 kHz, 89 kHz of operating source frequencies for the 81 kHz, 83 kHz, 85 kHz, 87 kHz, 89 kHz of primary and secondary resonance frequency variations. The secondary side capacitance is adjusted by VNA and, to change the primary resonance frequency, the primary side capacitance is changed.

To compare the measurement results with the theoretical calculations accurately, graphs are made same as Fig.

2. From Fig. 4, the yellow color range which represents the larger power factor values converge towards a point where the primary and secondary side resonance frequency are equal to the operating source frequency. However, the primary resonance frequency of the yellow color space is deviated from the primary resonance frequency of simulation results.

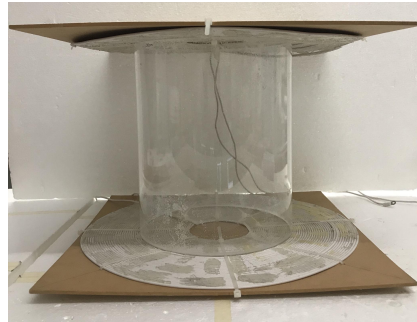


Fig. 3 Transmitting and receiving coil

### 3.3 Discussion

The larger input power factor values of Measurement result is almost given the similar result to the theoretical results for the WPT system with resonance frequency variation. As can be seen from both theoretical and measurement graphs, larger input power factor which is nearly equal to zero is obtained when operating source frequency and primary resonance frequency is nearly equal. However, the shape of input power factor of measurement results is different with the theoretical results. This unstable condition may be caused by

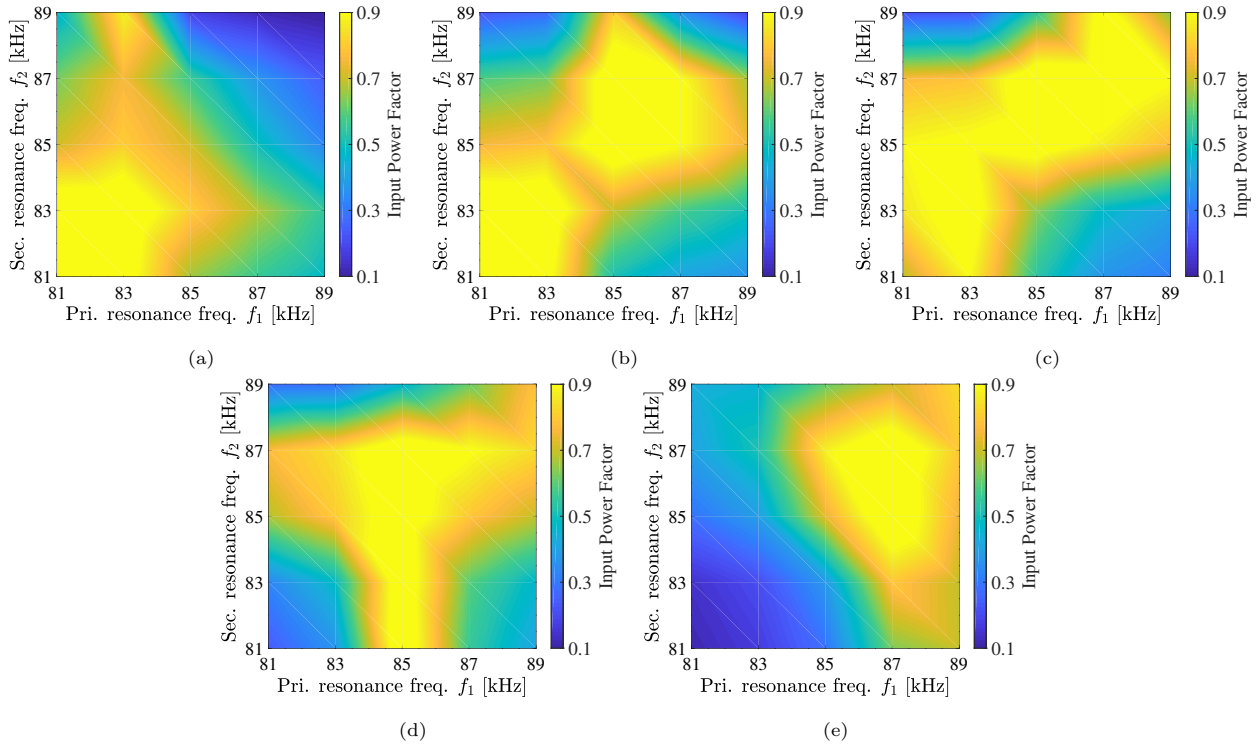


Fig. 4 Measurement results of transmission efficiency on resonance frequency mismatch.  
(a)  $f_0=81\text{kHz}$ , (b)  $f_0=83\text{kHz}$ , (c)  $f_0=85\text{kHz}$ , (d)  $f_0=87\text{kHz}$ , (e)  $f_0=89\text{kHz}$

because of neglecting the equivalent series resistances (ESRs) values of capacitors and the components.

#### 4. Conclusion

This paper presented on the input power factor variation on the WPT system with resonance frequency mismatch. The WPT circuit analysis is performed to examine the influence of source frequency, primary and secondary resonance frequency to input power factor. The Theoretical formula of the input power factor is expressed from the terms of operating frequency, primary and secondary resonance frequency. With that theoretical formula, the input power factor graphs are acquired when the resonance frequency mismatch occur. Finally, did the measurements to check the theoretical results for various resonance frequencies. It is confirmed that the input power factor is influenced by both primary and secondary resonance frequency. This time it was difficult to consider about the resistance of the capacitors. In the future works, resistance of the capacitors the load resistance variation will be considered.

#### Acknowledgment

This work was partly supported by JSPS KAKENHI Grant Number 16J06942 and 17H04915.

#### References

[1] Jia-Sheng Hu, Fei Lu, Chong Zhu, Chang-Yi Cheng, Sin-Li Chen, Tsai-Jiun Ren, Chris Mi, "Hybrid Energy Storage System of an Electric Scooter Based on Wireless Power Trans-

fer", *IEEE Transactions on Industrial Informatics*, Vol. 14, NO. 9, pp. 4169–4178, 2018.

- [2] Siqi Li and Chunting Chris Mi, "Wireless Power Transfer for Electric Vehicle Applications", *IEEE Journal of Emerging and Selected Topics in Power Electronics*, Vol. 3, No. 1, pp. 4–17, March 2015.
- [3] Takehiro Imura, Yoichi Hori, "Maximizing Air Gap and Efficiency of Magnetic Resonant Coupling for Wireless Power Transfer Using Equivalent Circuit and Neumann Formula", *IEEE Transactions on Industrial Electronics*, Vol. 58, No. 10, pp. 4746–4752, 2011.
- [4] Abhilash Kamini, Michael J. Neath, Adeel Zaheer, Grant A. Covic, John T. Boys, "Interoperable EV Detection for Dynamic Wireless Charging With Existing Hardware and Free Resonance", *IEEE Transactions on Transportation Electrification*, Vol. 3, No. 2, pp. 370–379, 2017.
- [5] Tommaso Campi, Silvano Cruciani, Francesca Maradei, Mauro Feliziani, "Near-Field Reduction in a Wireless Power Transfer System Using LCC Compensation", *IEEE Transactions on Electromagnetic Compatibility*, Vol. 59, No. 2, pp. 686–694, 2017.
- [6] Yeong H. Sohn, Bo H. Choi, Eun S. Lee, Gyu C. Lim, Gyu-Hyeong Cho, Chun T. Rim, "General Unified Analyses of Two-Capacitor Inductive Power Transfer Systems: Equivalence of Current-Source SS and SP Compensations", *IEEE Transactions on Power Electronics*, Vol. 30, No. 11, pp. 6030–6045, 2015.
- [7] Chunting Chris Mi, Giuseppe Buja, Su Y. Choi, Chun T. Rim, "Modern Advances in Wireless Power Transfer Systems for Roadway Powered Electric Vehicles," *IEEE Transactions on Industrial Electronics*, Vol. 63, pp. 6533–6545, June 2016.
- [8] Devendra Patil, Matthew K. McDonough, John M. Miller, Babak Fahimi, Poras T. Balsara, "Wireless Power Transfer for Vehicular Applications: Overview and Challenges," *IEEE Transactions on Transportation Electrification*, Vol. 4, pp. 3–37, December 2018.